Journal of the Korean Magnetic Resonance Society **2009**, *13*,64-83

Differential Diagnosis of Brain Diseases Using *In Vivo* Proton Magnetic Resonance Spectroscopy at 3 Tesla: A Preliminary Study

Yu-Lan Shen[1], Heoung-Keun Kang[1], Tae-Hoon Kim[2],
Thirunavukkarasu Sundaram[2], Hyeong-Jung Kim[2], Gwang-Woo Jeong[1,2*]

[1]*Department of Radiology and* [2]*Department of Biomedical Engineering*
Chonnam National University Medical School
Chonnam National University Hospital

Abstract : The purpose of this study was to evaluate the usefulness of *in vivo* 3T ^{1}H MRS with short TE for prescreening various brain diseases. Together with ten normal volunteers, 12 brain tumor patients(2 lymphomas, 5 malignant gliomas) and 5(benign meningiomas) and 10 brain ischemic disease patients(6 acute and 4 subacute infarctions) participated. Lymphomas showed increased intensities of Cho and Lac. Likewise, gliomas showed increased Cho and Lac, but with decreased NAA and β·γ-Glx; in higher grade of gliomas, Lac, Cho, mI and Lip predominantly increased with decrease of NAA. Benign meningiomas showed increased Cho, Lac and β·γ-Glx with decrease of NAA. The alanine peak at 1.47 ppm is a neuronal marker for meningiomas. Infarctions showed increased Lac and Lip and decreased NAA, α-Glx and β·γ-Glx where Lac increased with decrease of α-Glx in acute, and Cho, Lac and Lip increased with decrease of NAA in subacute. Elevated Lac and decreased NAA levels were more aggravated in subacute. Clinical application of the ^{1}H MRS with short TE at 3T is able to povide valuable spectral information for prescreening various brain diseases by monitoring the changes of disease-specific cerebral metabolite concentrations *in vivo*, and consequently, it can be applicable to assessment of differential diagnosis and malignancy as well.

Keywords: proton magnetic resonance spectroscopy (^{1}H MRS); brain diseases; differential diagnosis, malignancy

* To whom correspondence should be addressed. E-mail : gwjeong@jnu.ac.kr

INTRODUCTION

Recently, patients with cerebral disease along with population aging have steadily increased. Magnetic resonance imaging (MRI) is a non-invasive technique and its contrast in human brain images is much better than that of computed tomography [1, 2]. In addition, MRI for clinical applications has been used to distinguish pathological differences between normal tissue and tissue with disease [3, 4]. From a pathological point of view, metabolite changes within the cells occur prior to morphological and anatomical changes in the tissue [5]. However, MRI is difficult to measure quantitatively physiological and biochemical changes that lead to a pathology occurring at the cellular level [1, 6, 7].

A technique that overcomes this limitation is proton magnetic resonance spectroscopy (^{1}H-MRS) [7, 8]. *In vivo* ^{1}H-MRS has become an established technique for studies to evaluate biological systems because of high sensitivity and the ability to detect numerous metabolites [7-10]. Based on pathological phenomenon, the measurable metabolites determined with the use of *in vivo* MRS can especially provide useful physiological and biochemical information. With the use of MR spectroscopy [5, 11-15], determination of changes of biochemical metabolites may provide greater information concerning tissue characterization for evaluation of neuropathological disorders.

For a 1.5 Tesla (T) MR scanner, the major metabolites *in vivo* ^{1}H MRS can be evaluated at each concentration by integration of the peak areas of resonance frequency [13, 16]. Despite development of the MRS techniques and spectral deconvolution method [5, 12, 17-20], spectra for *in vivo* ^{1}H MRS include the presence of numerous unresolved multiplet groups with a low signal-to-noise ratio (SNR) such as glutamine and glutamate (Glx) and show heavy spectral overlap, which is especially severe at lower magnetic field strengths that are commonly used for clinical applications in humans [21]. Especially, the Glx metabolites, which are important in the evaluation of neuropathological disorders caused by a dysfunction in glutamatergic neurotransmission, were not clearly detectable on a ^{1}H MR spectrum with long echo time greater than about 50 millisecond [22-25].

Additional difficulties are the variable spectral patterns caused by magnetic susceptibility-induced distortions, and the presence of broad uncharacterized resonances from macromolecules, and unsuppressed water peak [21, 26]. For qualitative and quantitative

analyses, the observable metabolites on 1.5 T spectra still entail great difficulties [21]. Moreover, shimming the field in the region of interest (ROI) to the resonance of water assures the homogeneity of the field. Therefore, a homogenous magnetic field and high magnet strength are important prerequisites to obtain resolvable spectra.

In this study, we used a single-voxel ^{1}H MRS with short echo time to evaluate and to discriminate various brain diseases. In addition, *in vivo* MRS was performed at a 3 T magnet field strength to obtain spectra with high resolution and SNR. Our study was designed to evaluate the use of *in vivo* ^{1}H MRS to assess the differential diagnosis of brain tumors and other brain diseases.

MATERIALS AND METHODS

Subjects

The experimental subjects consisted of ten normal volunteers (five males and five females; mean age, 23 years) and 22 patients with brain disease (11 males and 11 females; mean age, 52 years) of which 12 patients had a tumor and ten patients had ischemic disease. For this study, the brain tumors included two lymphomas, five malignant gliomas and five benign meningiomas. Ischemic disease included six cases of acute infarction and four cases of subacute infarction. Exclusive criteria in normal volunteers included any illness and symptoms in the brain. Inclusive criteria for patients with a tumor were confirmed from a pathological diagnosis post surgery and for patients with ischemic disease, confirmation occurred after follow-up. All subjects submitted informed written consent prior to participation in this study. The study protocol was approved by the Chonnam National University Hospital (CNUH) Institutional Review Board (IRB).

MR imaging and MR spectroscopy

MRI and *in vivo* ^{1}H MRS were performed on a 3 T MR system (3T Magnetom Tim Trio MR Scanner; Siemens Medical Solutions, Erlangen, Germany) with a birdcage head coil. First, both T1 weighted images (T1WI) and T2 weighted images (T2WI) were acquired to provide reference anatomical images. After obtaining scout images, T1WI were acquired

with a TR/TE = 700/8 ms and T2WI were acquired with the following parameters: TR/TE = 4000/90 ms, field of view (FOV) = 220 × 170 mm^2, matrix size = 192 × 192, slice thickness = 5 mm, slice gap = 2 mm and total scan time = approximately 5 minutes.

Second, ^{1}H MRS was obtained with a PRESS (TR/TE = 2000/30 ms) pulse sequence. After automatic shimming and gradient tuning, water suppression was accomplished with three 60 Hz bandwidth chemical-shift-selective saturation (CHESS) pulses followed by spoiling gradients at the beginning of PRESS acquisition [5, 7] . Parameters for *in vivo* MRS were as follows: matrix size = 256 × 256, number of acquisitions = 96, voxel size = 8 (2×2×2) cm^3, spectral width = 1000 Hz, data points = 1024 and total scan time = 3 min 20 seconds.

After acquiring both the T1WI and T2WI, diffusion-weighted imaging (DWI) was also performed using spin-echo EPI pulse sequence with TR/TE = 5200/90ms, and b factor of 1000 s/mm^2.

Post-processing

After all data acquisition, raw data post-processing of free induction decay (FID) involved the following steps. First, zero-filling with one time (extended vector size: 2048) and apodization with a 2.5 Hz Gaussian filter were performed to increase the SNR. The time domain of FID was transformed to a frequency domain using Fourier transformation. Second, the baseline of a spectrum was corrected by the use of use six-polynomial fitting. Phase correction according to each spectrum used independent values to adjust phasing as changing values of the first order (constant order) and second order (linear order).

Quantification and statistical analysis

The MRI findings were assessed on the basis of an agreed consensus by two radiologists. The ^{1}H MR spectra were analyzed based on an agreed consensus between two radiologists and two MRS physicists. For ^{1}H MRS, the major seven metabolites in the human brain were assigned as follows: *N*-acetyl aspartate (NAA, 2.02 ppm), creatine (Cr, 3.02 ppm), choline (Cho, 3.20 ppm), *myo*-inositol (mI, 3.56 ppm), lactate (Lac, 1.30 ppm), lipid (Lip, 0.91ppm), α-glutamate/glutamine (α-Glx, 3.60–3.80 ppm), β·γ-glutamate/

glutamine (β·γ-Glx, 2.20–2.50 ppm). The Cr peak was used as a standard to normalize the signal intensities of the metabolites.

Quantitative analysis was performed with an MR spectroscopy data analysis package of a Leonardo syngo MR 2005A workstation (Siemens Medical Solutions) with a non-linear least square fitting algorithm that operated in the time domain (FID signal) as implemented in the syngo MR package. In addition, changes of the metabolite concentration in patient were calculated on the basis of the normal brain.

Statistical analyses were performed with statistical package for the social science (SPSS) version 14.0 to determine the difference in the levels and ratio of metabolites between the normal volunteers and patients with brain disease using the Mann-Whitney U test.

RESULTS

Diagnostic view of MRI features

Fig. 1 shows the axial T2 weighted images including the volume of interest (VOI) acquired from normal volunteers and patients with brain disease. Lymphomas (Fig. 1b) were observed in the thalamus and white matter of the parietal lobe. Especially, lymphomas and the brain parenchyma as seen on T2WI showed equivalent signal intensities and perilesional edema for the abnormal lesions. With enhancement, the lesions were well defined whereas the necrosis regions were obscure. Therefore, it was difficult to discriminate macrographically the difference between malignant gliomas and metastatistic tumors.

For malignant gliomas, oligodendrogliomas (low grade; Fig. 1c) as seen on T2WI showed equivalent signal intensity in the normal grey matter and in the abnormal lesions. In addition, oligodendrogliomas (grade II) showed weak enhancement and perilesional edema in the abnormal lesions. Gliomas (high-grade; Fig. 1d) were observed in the white matter of the skull based and frontal lobe. Gliomas (grade IV) as seen on T2WI showed high signal intensity. These tumors also showed strong enhancement and severe edema. However, in one of three patients, it was difficult to discriminate a glioma, as the presence of perilesional edema was equivocal.

For benign meningiomas (Fig. 1e), high signal intensity in the abnormal lesions was seen on T2WI. With enhancement, meningiomas showed strong homogeneous enhancement and the epidural tail formed that surrounded the abnormal lesions was helpful for diagnosis.

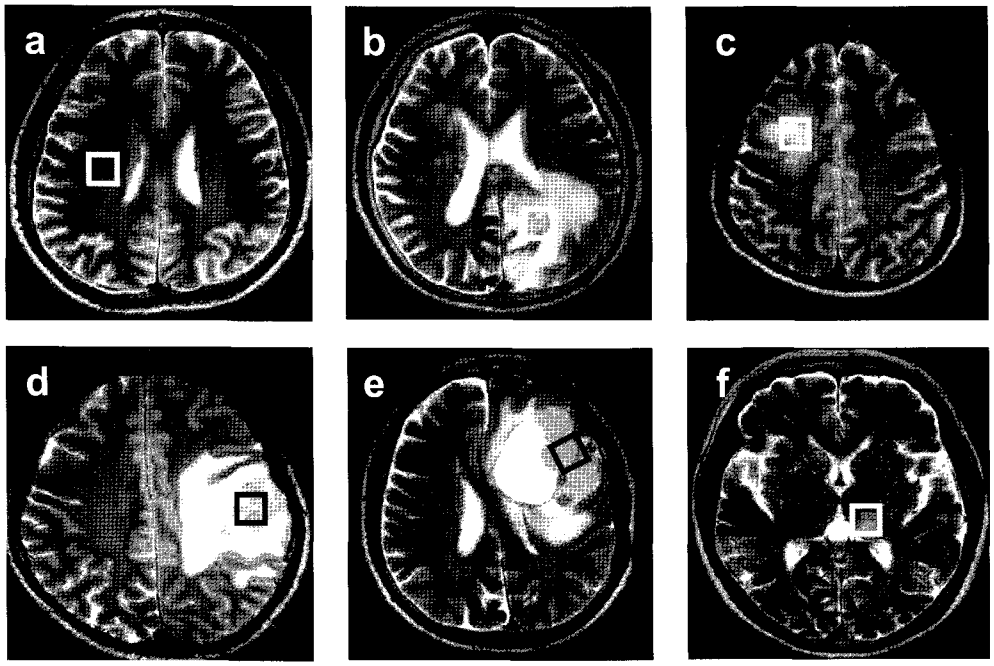

Fig. 1. Axial T2 weighted MR images with the volume of interest (VOI) for *in vivo* MR spectroscopy, which were acquired from a normal volunteer (a) and patients with lymphoma (b), oligodendroglioma (c), glioblastoma (d), benign meningioma (e) and acute infarct (f).

Fig. 2 demonstrates the T2WI and DWI for patients with brain infacrtions. In four patients with an acute infarction and four patients with a subacute infarction, the lesions showed high signal intensities as seen on T2WI and DWI (Fig. 2 a-b and c-d). Therefore, it was easy to discriminate the abnormal lesions. However, in two cases of acute infarction, it was difficult to discriminate the abnormal lesions as equivocal signal intensities were observed on T2WI. It was possible to discriminate among the abnormal lesions with the use of DWI (Fig. 2 e-f and g-h).

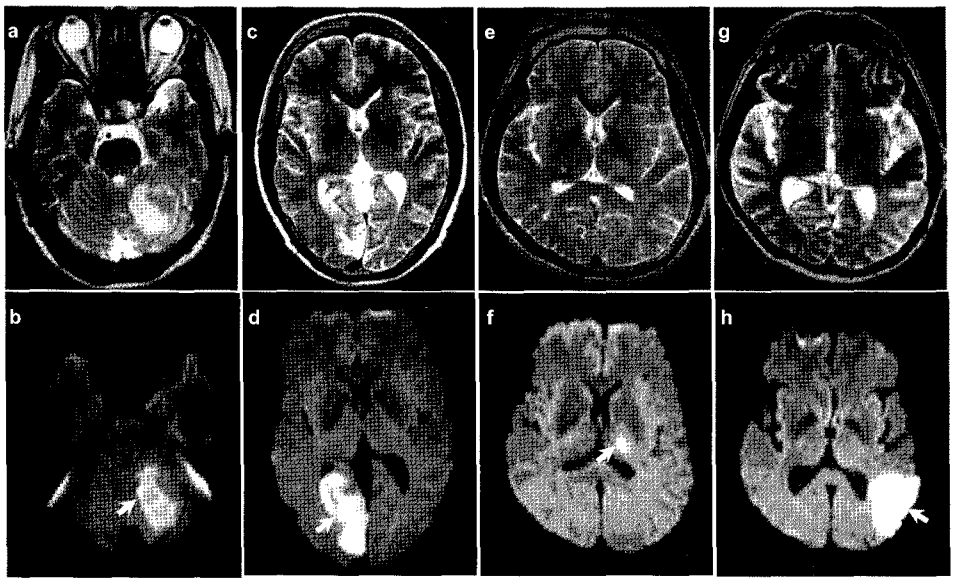

Fig. 2. Axial T2-weighted MR images (upper) and diffusion weighted images (lower) from patients with acute infarction. In a 52-year-old woman (a and b) within six hours of the onset of the infarction, T2WI and DWI show the infracted region in the left cerebellum. In a 63-year-old woman (c and d) within 20 hours of the onset of the infarction, T2WI and DWI show the infarcted region in the right calcarine gyrus. However, in a 46-year-old man (e and f) within six hours and in a 63-year-old man (g and h) within nine hours of the onset of the infarction, only DWI discriminates the infarcted region in the left thalamus and in the left parietal gyrus.

In vivo ^{1}H MRS features and brain metabolite changes

Fig. 3 demonstrates MR spectra that were respectively acquired from normal volunteers and patients with brain disease, including patients with lymphomas, oligodendrogliomas, gliomas, benign meningiomas and acute infarctions.

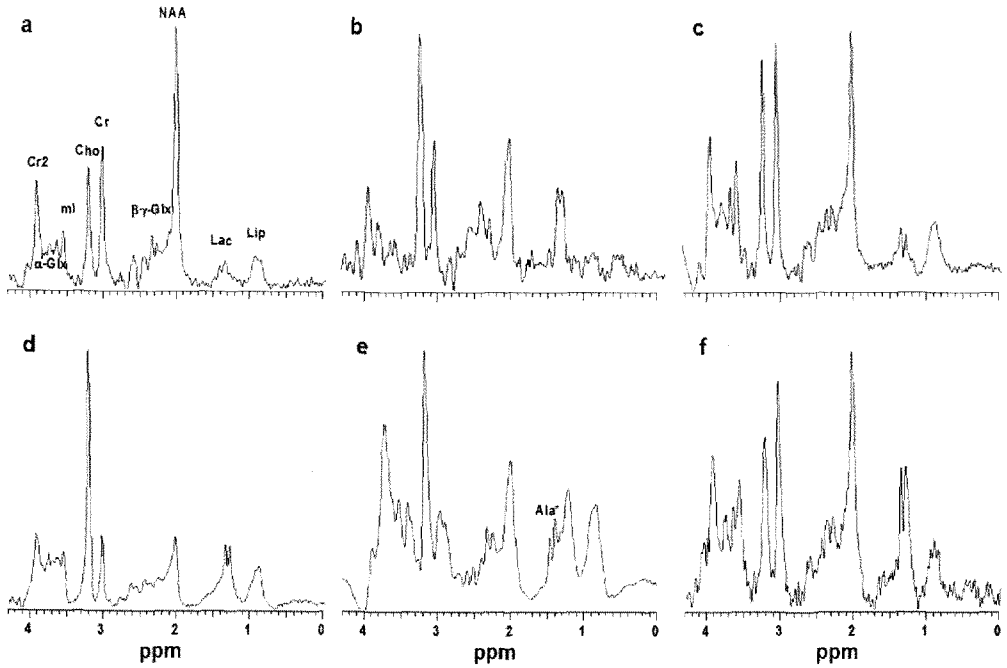

Fig. 3. Proton MR spectra acquired from a normal volunteer (a) and patients with lymphoma (b), oligodendroglioma (c), glioblastoma (d), benign meningioma (e) and acute infarct (f).

Table 1 shows the metabolite intensity ratios in normal volunteers and in patients with various types of brain disease. Fig. 4 shows the changing rate of brain metabolites in patients with different diseases as compared with the normal volunteers.

As compared with the normal volunteers, patients with lymphomas (Fig. 4b) show increases in the metabolite intensity ratios of Cho/Cr, Lac/Cr and β·γ-Glx/Cr 99%, 704% and 21%, respectively, while NAA/Cr, mI/Cr, Lip/Cr and α-Glx/Cr decreased by 19%, 28%, 13% and 9%, respectively.

Metabolite intensity ratios	Normal brain* (N) (n=10)	Lymphoma (L) (n=2)	The ratio† of increase/ decrease (L vs. N)	Glioma (G) (n=5)	The ratio of increase/ decrease (G vs. N)	Meningioma (M) (n=5)	The ratio of increase/ decrease (M vs. N)	Infarction (I) (n=10)	The ratio of increase/ decrease (I vs. N)
NAA/Cr	1.86±0.21	1.51±0.34	-18.82	1.43±0.23	-23.12	1.21±0.40	-34.95	1.49±0.40	-19.89
Cho/Cr	0.94±0.09	1.87±0.47	98.94	2.06±0.77	119.15	1.25±0.22	32.98	1.07±0.34	13.83
mI/Cr	0.46±0.11	0.33±0.25	-28.26	0.60±0.19	30.43	0.48±0.31	4.35	0.62±0.45	34.78
Lac/Cr	0.23±0.04	1.85±0.76	704.35	1.28±0.67	456.52	0.37±0.17	60.87	2.01±1.30	773.91
Lip/Cr	0.60±0.11	0.52±0.55	-13.33	0.94±0.31	56.67	0.86±0.39	43.33	0.80±0.36	33.33
α-Glx/Cr	1.02±0.15	0.92±0.23	-9.80	1.01±0.43	-0.98	1.13±0.40	10.78	0.83±0.25	-18.63
β·γ-Glx/Cr	1.46±0.21	1.76±0.01	20.55	1.09±0.38	-25.34	0.84±0.20	-42.47	1.10±0.50	-24.66
Alanine/Cr	-	-	-	-	-	0.71±0.36	-	-	-

* Average of the metabolite intensity ratios of white matter and grey matter in normal brain

† The ratio of increase/decrease = Metabolite ratio $_{(Abnormal - Normal)}$ / Metabolite ratio $_{(Normal)}$ × 100

Table 1. Metabolite Intensity Ratios in the Normal Brain and for Various Brain Diseases

In patients with malignant gliomas (Fig. 4c and d), the metabolite intensity ratios of Cho/Cr, mI/Cr, Lac/Cr and Lip/Cr increased by 119%, 30%, 457% and 57%, respectively, while NAA/Cr, α-Glx/Cr and β·γ-Glx/Cr decreased by 23%, 1% and 25%, respectively. Table 2 compares the metabolite intensity ratios between normal volunteers and patients with low (I and II) and high (III and IV) gliomas. In patients with low grade gliomas, the metabolite intensity ratios of Cho/Cr and Lac/Cr increased by 49% and 109%, respectively, while NAA/Cr, mI/Cr, Lip/Cr, α-Glx/Cr and β·γ-Glx/Cr decreased by 37%, 15%, 8%, 9% and 46%, respectively. In patients with high grade gliomas, the metabolite intensity ratios of Cho/Cr, mI/Cr, Lac/Cr, Lip/Cr and α-Glx/Cr increased by 166%, 63%, 687%, 98% and 4%, respectively, while the NAA/Cr and β·γ-Glx/Cr ratios decreased by 14% and 12%, respectively.

In patients with benign meningiomas (Fig. 4e), the metabolite intensity ratios of Cho/Cr, mI/Cr, Lac/Cr, Lip/Cr and α-Glx/Cr increased by 33%, 4%, 61%, 43% and 11%, respectively, while NAA/Cr and β·γ-Glx/Cr decreased by 35% and 42%, respectively. It should be notice that the peak at 1.47 ppm represents alanine that is a neuronal marker of meningiomas, and the alanine/Cr ratio was 0.71 ± 0.36.

In patients with brain infarction (Fig. 4f), the metabolite intensity ratios of Cho/Cr, mI/Cr, Lac/Cr and Lip/Cr increased by 14%, 35%, 774% and 33% respectively, while NAA/Cr and α-Glx/Cr and β·γ-Glx/Cr decreased by 20%, 19% and 25%, respectively. Table 3 shows the metabolite intensity ratios in normal volunteers and patients with brain infarctions. In patients with acute infarctions, the metabolite intensity ratios of mI/Cr, Lac/Cr and Lip/Cr increased by 39%, 396% and 5%, respectively, while NAA/Cr, Cho/Cr, α-Glx/Cr and β·γ-Glx/Cr decreased by 6%, 10%, 27% and 27%, respectively. In patients with subacute infarctions, the metabolites of Cho/Cr, mI/Cr, Lac/Cr and Lip/Cr increased by 48%, 26%, 1348% and 75%, respectively, while the NAA/Cr, α-Glx/Cr and β·γ-Glx/Cr ratios decreased by 40%, 1% and 21%, respectively.

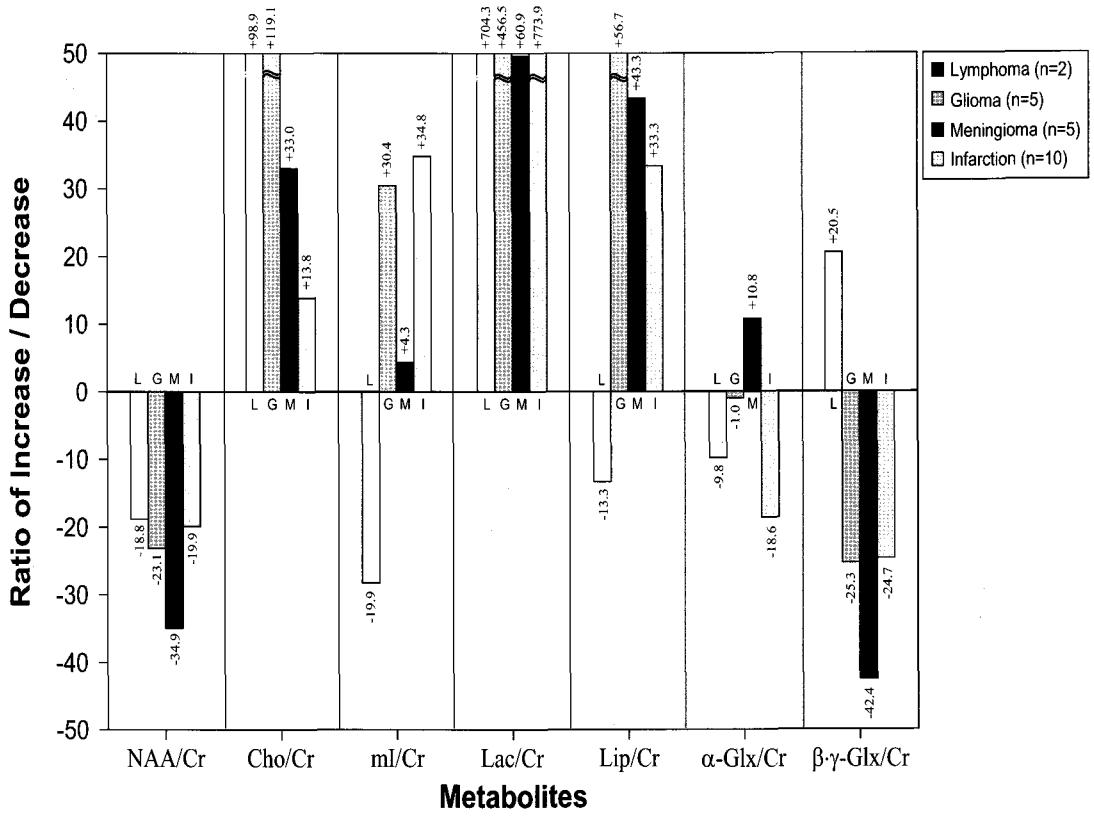

Fig. 4. The bar-graph shows the change ratios of the metabolite intensities between the normal volunteers and patients with various brain diseases.

Differential metabolites of various brain diseases

In Table 4 and Fig. 5, the significance of the metabolite intensity ratios showed a difference between normal volunteers and patients with various brain diseases based on the use of the Mann-Whitney U test ($p < 0.05$). Patients with lymphomas showed significantly increased Cho/Cr ($p = 0.022$) and Lac/Cr ($p = 0.021$) levels. Patients with gliomas showed significantly increased Cho/Cr ($p = 0.011$) and Lac/Cr ($p = 0.001$) with decreased NAA/Cr ($p = 0.002$) and β·γ-Glx/Cr ($p = 0.041$). For patients with low-grade gliomas, a significant difference was found with an increased Lac/Cr ($p = 0.021$) with a decreased NAA/Cr ($p = 0.002$). For patients with high-grade gliomas, a significant difference was found with

increased Cho/Cr (p = 0.006), mI/Cr (p = 0.020), Lac/Cr (p = 0.006) and Lip/Cr (p = 0.006) and a decreased NAA/Cr (p = 0.019). Patients with benign meningiomas showed significantly increased Cho/Cr (p = 0.006), Lac/Cr (p = 0.041) and β·γ-Glx/Cr (p = 0.001) with a decreased NAA/Cr (p = 0.014).

Metabolite intensity ratios	Lymphoma (L) p-value * (n=2)	Glioma (G) (n=5)		Meningioma (M) (n=5)	Infarction (I) (n=10)	
		Low grade (L) (n=2)	High grade (H) (n=3)		Acute (A) (n=6)	Subacute (S) (n=4)
NAA/Cr	.229	.002**		.014*	.016*	
		.022*	.019*		.377	.002**
Cho/Cr	.022*	.011*		.006**	.344	
		.390	.006**		.314	.003**
mI/Cr	.456	.163		.358	.930	
		.567	.020*		.831	.907
Lac/Cr	.021*	.001***		.041*	.000***	
		.021*	.006**		.000***	.002**
Lip/Cr	.954	.077		.518	.036*	
		.647	.006**		.259	.024*
α-Glx/Cr	.529	.518		.496	.007**	
		.909	.437		.001***	.535
β·γ-Glx/Cr	.067	.041*		.001***	.028*	
		.110	.144		.107	.438

* Mann-Whitney U test; All patients with tumors and ischemic diseases compared with normal voluneers (n=10)
: * p < 0.05, ** p < 0.01, *** p < 0.001.

Table 4. Comparison of the Differential Metabolite Ratios in Various Brain Diseases

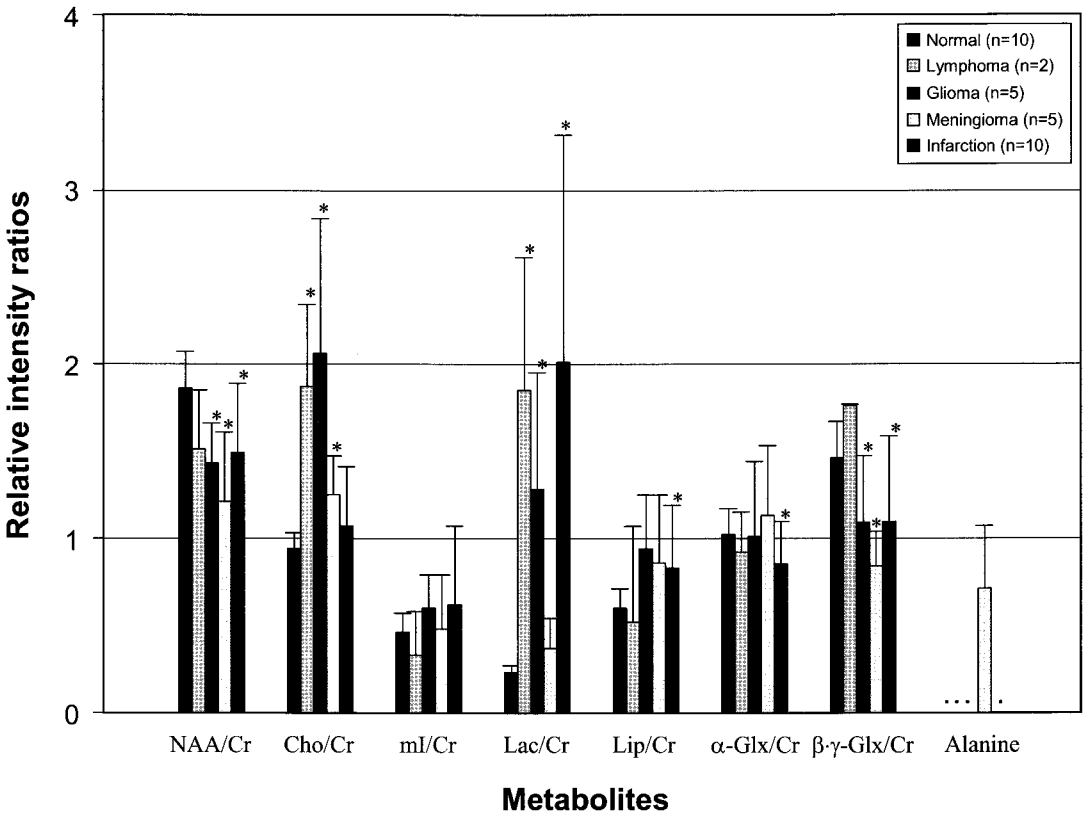

Fig. 5. The bar-graph compares the metabolite intensity ratios between normal subjects and patients with various brain diseases. The asterisks show significant difference of the metabolite intensity ratios (p<0.05).

For patients with both acute infarctions and subacute infarctions, a significant difference for patients with both types of infarctions was found with increased Lac/Cr (p = 0.000) and Lip/Cr (p = 0.036) and decreased NAA/Cr (p = 0.016), α-Glx/Cr (p = 0.007) and β·γ-Glx/Cr (p = 0.028). Patients with an acute infarction showed a significantly increased Lac/Cr (p = 0.000) with a decreased α-Glx/Cr (p = 0.001). Patients with a subacute infarction showed significantly increased Cho/Cr (p = 0.003), Lac/Cr (p = 0.002) and Lip/Cr (p = 0.024) and a decreased NAA/Cr (p = 0.002). Elevated Lac and decreased NAA levels were detected in patients where the subacute infarction was more aggravated, and patients with both types of infarctions had increased Cho/Cr and Lac/Cr and a decreased NAA/Cr.

DISCUSSION

Today, 3T is becoming a standard MR system in routine clinical applications. The advantages of higher field strength are increases of SNR and spectral resolutions. Barker *et al.* [27] reported that the MRS signal intensity using a STEAM pulse sequence with a short TE at 3 T increased by 28% than at 1.5 T, and as a result, metabolite peaks of Cho and NAA increased. Bartha *et al.* [26] reported that the signal intensity of NAA *in vivo* ^{1}H MRS at 4 T increased by 25% over 1.5 T. With 3 T high magnet field strength, our study showed enhanced spectral resolution and SNR, and thus assignment and quantification of metabolites are more accurately analyzed as compared with 1.5 T. In spite of these improvements, however, for unresolved multiplets and spectral overlaps with distorted baseline remained [5, 13]. In this study, the major brain metabolites were quantitatively evaluated with criterion that the signal intensities of the Cr metabolite were stable over the normal and abnormal tissues, and thus the intensities of metabolites were normalized with the intensity of Cr [21, 25, 28].

The NAA is the major component of neuron, and thus NAA levels were correlated with neuronal and axonal densities [29]. The NAA metabolite is closely related with diseases including tumors as well as neuronal loss, degeneration and inflammation [29, 30]. Clark [31] reported that NAA synthesis is related with mitochondrial energy metabolism, and NAA loss may in some cases be reversible, but if the mitochondrial dysfunction is prolonged, irreversible damage may follow and be ultimately reflected in neuronal loss. Therefore, the level of NAA metabolite in patients with a neuronal diseases can be considered as a diagnostic marker that reflects neuronal and mitochondrial function within neurons [29, 30]. Ott *et al.* [32] reported that NAA levels in high-grade gliomas tended to decrease more than low-grade gliomas. However, MRS with the use of a long TE is difficult to determine a precise diagnosis of tumor pattern. Gillard *et al.* [24] reported that NAA levels in patients with an acute infarction showed a slight decrease. In our study, compared with normal range of 1.86 $\pm$ 0.21 of the NAA/Cr metabolic ratio, patients with infarction showed a slight decrease of 1.49 $\pm$ 0.40 and patients with lymphomas, gliomas and meningiomas showed a greater decrease of 1.51 $\pm$ 0.34, 1.43 $\pm$ 0.23 and 1.21 $\pm$ 0.40, respectively. In addition, the NAA/Cr ratios decreased in patients with all types of lesions and showed a significant difference for

all of the lesions except lymphomas ($p < 0.05$). Our findings are consistent with findings of a previous study [33] that showed decreased NAA/Cr ratios with progression of neurofibrillary abnormalities. Therefore, we presume that a decrease in the NAA/Cr ratio is correlated with neuronal damage and/or loss. For a decreased NAA/Cr ratio, an aberration or an abnormality from a spectrum might suggest that MR images can depict anatomic degeneration. The finding of a decreased NAA/Cr for a cerebral disease suggests two processes: the first process is actual neuronal death and the other process is a decreased level of functionality or metabolic integrity in the neurons.

The Choline peaks result mainly from an emerging increase of the steady state levels of the sum of phophorylcholine and glycerophosphorylcholine. Breakdown of the choline containing cell membrane results in an increase of the intensity of Cho [30]. In *in vitro* studies, the total Cho concentration has been confirmed to correlate highly with the levels of free choline and glycerophosphorylcholine. In particular, loss of cholinergic neurons predicts the proportion of soluble free choline and glycerophosphorylcholine [34, 35]. Choline has not been used as a neuronal marker to decide the grade of a tumor; however, the level of the Cho metabolite is useful to identify the grade of tumors [34, 35]. In the present study, as compared with the normal volunteers, the levels of Cho in patients with lymphomas, gliomas and benign meningiomas increased by 98%, 119% and 37%, respectively. In patients with a subacute infarction, the Cho level increased by 48%, while the Cho decreased by 10% in patients with an acute infarction. With decreased NAA level in patients with all types of cerebral lesions, the Cho showed a different pattern in patients with abnormal lesions, except for patients with an acute infarction. Due to the result of growth of abnormal tissue such as a tumor, disorder of intracellular neuronal transmission is able to infer a change of the Cho signal intensity within abnormal cell. Therefore, our findings support that levels of NAA and Cho are the important metabolites associated with neuronal function.

Lactate is a product produced by anaerobic glucolysis. Increased Lac levels imply deficient oxygen and an ischemic condition in tissue. Together with a decreased NAA and increased Cho levels, an increased Lac level is associated with a high grade of a malignant tumor. Meyerand *et al*, [36] reported that the signal intensity of Lac tends to increase with an ascending grade of a malignant tumor. Also, Kuesel *et al.* [37] reported that Lac levels were especially increased in high-grade gliomas and necrotic regions as well. Our findings are

consistent with the results reported by Meyerand *et al.* [36]. As compared with the normal volunteers, the Lac level in patients with lymphomas, gliomas and meningiomas increased by 704%, 456% and, 60%, respectively. For patients with acute and subacute infarction, the Lac level increased by 395% and 1348%, respectively. This finding suggests that it is difficult to supply sufficient oxygen in the lesions due to intraarterial thrombosis causing the ischemic condition within the tissue of a lesion.

The *myo*-inositol is recognized as an important osmolyte and strocyte marker [30]. Gliosis in the central nervous system (CNS) results from a proliferation of astrocytes with damage by inflammatory CNS demyelination [30]. Therefore, astrocytes are the most important histopathological sign of a CNS injury. For this reason, elevation of the mI level may be related to gliosis in the brain of patients with various types of tumors and ischemic disease. In patients with Alzheimer's disease [33], mI level increased and NAA level decreased. The increase of the mI level may be due to the inhibitory mechanism of the enzyme that converts phosphatidyl inositol [33] . However, decreased levels of mI have been shown in patients with mania when lithium is administered and in patients with diabetic neuropathies [38]. In the present study, patients with gliomas showed a 30% increase of the mI level as compared to the normal volunteers. The mI level in patients with benign meningiomas was observed in the normal range. Patients with an acute infarction (within 24 hours) and a subacute infarction (within 1–7 days) showed increases of 39% and 26% in the mI level, respectively, and were accompanied with decreases of 6% and 40% in the NAA level, respectively. Our findings suggest that a change in the mI/Cr ratio precedes a decrease of the NAA/Cr ratio.

The main biological functions of lipids include energy storage, acting as structural components of cell membranes and participation as important signaling molecules. The signal of the macromolecule lipid is invisible in MRS until its liberation into small molecules by some severe pathological process. Michaelis *et al.* [39] reported that level of Lip in patients with malignant gliomas and meningiomas increased. In our study, the Lip level in patients with gliomas, meningiomas and infarctions increased by 57%, 43% and 33%, respectively, and the findings were consistent with those of the previous study [39] . Contrary to our expectation, however, the Lip level in patients with lymphomas decreased by 13%.

Glutamate is the most abundant neurotransmitter in the brain and it plays a central role in nitrogen metabolism and participates in multiple biochemical pathways [22, 30]. Released glutamate is taken up by glial cells, where it is converted to glutamine, transported back to presynaptic neurons and is reconverted to glutamate [23]. Glutamine, a product of the amination of glutamate, is transferred to neurons from glial cells after the exocytotic release of glutamate into the synaptic space [22]. Thus, it seems that the glutamate-glutamine cycle plays a role for neuron-glia communication in the synapse, and that impairment of the glutamate-glutamine cycle may be implicated in psychiatric pathophysiology [23]. Especially in the short-term, synaptic release of glutamate determines cognitive processes; abnormal continuous release of glutamate may play a role in acute neuronal death, such as that observed in stroke and in the pathogenesis of chronic neurodegenerative disorders [24]. Several lines of evidence suggest that a dysfunction in glutamatergic neurotransmission might be involved in the pathophysiology of schizophrenia [23]. With the use of *in vivo* ^{1}H MRS acquired with a short TE (30 ms) at 3.0 T, quantification of the α-Glx/Cr and β·γ-Glx/Cr peaks depicted on spectra was more reliable because of enhanced spectral resolution. The α-Glx/Cr level in patients with menigiomas increased, while the α-Glx/Cr in patients with other diseases decreased. The α-Glx/Cr level only showed a significant difference in patients with an infarction ($p < 0.01$). In addition, the β·γ-Glx/Cr level increased in patients with lymphomas, whereas its level decreased in patients with other diseases. It is important to note that the β·γ-Glx/Cr level showed a significant difference in patients with gliomas ($p < 0.05$), meningiomas ($p < 0.001$) and infarctions ($p < 0.05$), respectively (Tables 1 and 4).

Based on the findings in a study by Castillo *et al.* [22], lipid increased in malignant tumors reflecting necrotic processes. Especially, only an increased Lip/Cr level may discriminate the difference between a lymphoma and a glioma. However, in the present study, patients with lymphomas showed decreased Lip/Cr level accompanied with decreased NAA/Cr and mI/Cr and increased Cho/Cr and Lac/Cr levels.

In patients with gliomas, the NAA/Cr level generally decreased, while the levels of Cho/Cr and Lac/Cr increased. Our results are consistent with those of the previous studies [36, 40]. A decreased NAA level reflects a loss of neural cells, and increased Cho and Lac levels suggest a change in membrane synthesis and hypoxia, respectively, within malignant tumor cells. In patients with benign meningiomas, the levels of NAA and β·γ-Glx decreased, while

the levels of Cho/Cr, Lac/Cr, Lip/Cr and α-Glx/Cr increased. In this study, a doublet of alanine at 1.47 ppm was observed with the level of 0.71 ± 0.47. Alanine is a nonessential amino acid and is most commonly produced by reductive amination of pyruvate. Therefore, the alanine peak can be considered as a specific neuronal marker of meningiomas.

An infarction is a well known disease of neuronal disruption that is caused by a decrease of blood flow of a local region or a whole region in the brain [24] . In patients with an infarction, previous studies [12, 24] showed increased Lac with decreased NAA level. It should be noted that increased Cho level was observed in our study.

Our current study involves several limitations. First, the present study dealed with a small number of subjects, which may reduce the predictive power of ^{1}H-MRS. A second limitation involves the accuracy of localization of the focal lesion, which is free of contamination from outside. This limitation becomes more severe when the abnormal lesions were positioned adjacent to the sellar region or grey matter surrounding the ventricle and skull. In spite of the use of automatic and manual shimming for a homogeneous magnetic field, it was difficult to avoid magnetic susceptibility effects.

In spite of such limitation in our study, however, our findings provide valuable spectral information for prescreening various brain diseases by monitoring the changes of disease-specific cerebral metabolites *in vivo*, and consequently, it can be applicable to assessment of differential diagnosis and malignancy as well.

CONCLUSIONS

In summary, ^{1}H MRS with short TE at 3T provides more reliable spectral information for monitoring the changes of disease specific cerebral metabolite concentrations *in vivo*, and consequently, it can be applicable to the assessment of differential diagnosis and malignancy as well.

Acknowledgements

This study was financially supported by the research fund of Chonnam National University (2003).

REFERENCES

1. Bihan D. L., *Invest Radiol.* **27**, 6-11 (1992)
2. Kim S. Y., Woo D. C., Bang E. J., et al. *J. Kor Magn Reson.* **12**, 14-25 (2008)
3. Damadian R., *Science* **171**, 1151-53 (1971)
4. Tovi M, Thuomas K. A., Bergström K., et al. *Acta Radiologica Supplementum* **369**, 161-63 (1986)
5. Barker P. B., Lin D. D. M., *Prog Nucl Magn Reson Spectrosc.* **49**, 99-128 (2006)
6. Chiang I. C., Kuo Y. T., Lu C. Y., et al. *Neuroradiology* **46**, 619-27 (2004)
7. Cousins J. P., *Am J Roentgenol.* **164**, 1337-47 (1995)
8. Braunová Z., Kasparová S., Mlynárik V., et al. *Cell Mol Neurobiol.* **20**, 703-15 (2000)
9. Laptook A. R., Corbett R. J., Sterett R., Garcia D., Tollefsbol G., *Pediatr Res.***38**, 919-25 (1995)
10. Weiner M. W., *Invest Radiol.* **23**, 253-61 (1988)
11. Howe F. A., Maxwell R. J., Saunders D. E., Brown M. M., Griffiths J. R., *Magn Reson Q.* **9**, 31-59 (1993)
12. Sappey-Marinier D., Calabrese G., Hetherington H. P., et al. *Magn Reson Med.* **26**, 313-27 (1992)
13. Burtscher I. M., Skagerberg G., Geijer B., Englund E., Stahlberg F., Holtas S., *Am J Neuroradiol* **21**, 84-93 (2000)
14. Poptani H., Gupta R. K., Roy R., Pandey R., Jain V. K., Chhabra D. K., *Am J Neuroradiol* **16**, 1593-603 (1995)
15. Weybright P., Sundgren P. C., Maly P., et al. *Am J Roentgenol* **185**, 1471-76 (2005)
16. Choi C. B., Hong S. T., Choe B. Y., et al. *J Kor Magn Reson.* **10**, 105-14 (2006)
17. Jeong G.. W., Kang H. K., *Concepts Magn Resonance* **18A**, 146-156 (2003)
18. Overloop K., Van Hecke P., Vanstapel F., et al. *NMR Biomed.* **9**, 315-21 (1996)
19. Radda G. K., Rajagopalan B., Taylor D. J., *Magn Reson Q.* **5**, 122-51 (1989)
20. Christiansen P., Henriksen O., Stubgaard M., Gideon P., Larsson H. B., *Magn Reson Imaging* **11**, 107-18 (1993)
21. Bottomley P. A., *Radiology* **170**, 1-15 (1989)
22. Castillo M., Kwock L., Mukherji S. K., *AJNR Am J Neuroradiol* **17**, 1-15 (1996)

23. Hashimoto K., Engberg G., Shimizu E., Nordin C., Lindström L. H., Iyo M., *BMC Psychiatry* **5**, 6-10 (2005)
24. Gillard J. H., Barker P. B., van Zijl P. C., Bryan R. N., Oppenheimer S. M., *Am J Neuroradiol* **17**, 873-86 (1996)
25. Barker P. B., *Seminars in Cerebrovascular Diseases and Stroke* **1**, 331-42 (2001)
26. Bartha R., Drost D. J., Menon R. S., Williamson P. C., *Magn Reson Med.* **44**, 185-92 (2000)
27. Barker P. B., Hearshen D. O., Boska M. D., *Magn Reson Med.* **45**, 765-69 (2001)
28. Weybright P., Maly P., Gomez-Hassan D., Blaesing C., Sundgren P. C., *Neuroradiology* **46**, 541-49 (2004)
29. Barker P. B., *Ann Neurol* **49**, 423-24 (2001)
30. Danielsen E. R., Ross B., *Magnetic Resonance Spectroscopy Diagnosis of Neurological Diseases. New York, Basel MARCEL DEKKER, INC.* **6**. (1999)
31. Clark J. B., *Developmental Neuroscience* **20**, 271-76 (1998)
32. Ott D., Hennig J., Ernst T., *Radiology* **186**, 745-72 (1993)
33. Kantarci K., Knopman D. S., Dickson D. W., et al. *Radiology* **248**, 210-20 (2008)
34. Tien R. D., Lai P. H., Smith J. S., Lazeyras F., *Am J Roentgenol* **167**, 201-09 (1996)
35. Negendank W. G., Sauter R., Brown T. R., Evelhoch J. L., Falini A., *J Neurosurg.* **84**, 449-58 (1996)
36. Meyerand M. E., Pipas J. M., Mamourian A., Tosteson T. D., Dunn J.F., *Am J Neuroradiol* **20**, 2-3 (1999)
37. Kuesel A. C., Sutherland G. R., Halliday W., Smith I. C., *NMR Biomed.* **7**, 149-55 (1994)
38. Maxwell R. J., Martínez-Pérez I., Cerdán S., et al. *Magn Reson Med.* **39**, 869-77 (1998)
39. Michaelis T., Merboldt K. D., Bruhn H., Hanicke W., Frahm J., *Radiology* **187**, 219-27 (1993)
40. Kwock L., Smith J. K., Castillo M., et al. *Technol Cancer Res Treat.* **1**, 17-28 (2002)